

UDC 528.852.088.3

doi: 10.32620/reks.2022.3.13

Galina PROSKURA, Oleksii RUBEL, Vladimir LUKIN

National Aerospace University "Kharkiv Aviation Institute", Kharkiv, Ukraine

ON CLASSIFIER LEARNING METHODOLOGIES WITH APPLICATION TO COMPRESSED REMOTE SENSING IMAGES

*Remote sensing images have found numerous applications nowadays. A traditional outcome or intermediate result of their processing is a classification map. Such maps are usually obtained from a pre-trained classifier and it is desired to have the produced classification maps as accurately as possible. The basic **subject** of this article is the factors determining this accuracy. The main among them are the quality of remote sensing data and classifier type, parameters and training approach. Image quality can be degraded due to several factors. One of them is distortions introduced by lossy compression that is widely used due to a huge volume of acquired data and the necessity to sufficiently decrease their size at transmission, storage and/or dissemination stages. Because of this, the main **goal** of this paper is to consider classification and lossy compression jointly. In particular, this means that the classifier learning can be performed for original (uncompressed, compressed in a lossless manner) images (if they are available) as well as for compressed data at hand (offered to a user for classification and further analysis). The **task** of this paper is to consider and compare these two options. The first one is the classifier learning for original images and further application to compressed data, where images can be compressed with different compression ratios while producing compressed data of different quality. The second option is the use of the classifier learning for compressed images, where compression parameters for training data can be approximately the same as for the images to which the classifier is applied. The main **result** is that the latter methodology can provide certain benefits compared to the classifier learning for original data if one has to classify compressed remote sensing data. Simulation data are obtained for a classifier based on a convolutional neural network. As images for training and verification, four real-life three-channel (visible range) Sentinel-2 remote sensing images of Kharkiv and Kharkiv region are employed that possess different complexity of the content and have four main classes. The practical recommendations are given. In **conclusion**, we can state that it is worth having classifiers trained for several degrees of compression and it is reasonable to compress complex structure images with special care.*

Keywords: *lossy compression; three-channel images; classification; neural network classifier; training data.*

1. Introduction

Nowadays, remote sensing (RS) from satellites and airborne carriers including unmanned aerial vehicles and drones have found numerous applications including forestry, ecological monitoring, precision agriculture [1, 2], etc. Images produced by different sensors have to be processed where processing includes a wide set of possible operations (stages) including georeferencing, calibration, denoising or deblurring, classification [3 - 6] and so on. RS data classification is a typical image processing stage [6 - 8] that can be either final or intermediate (pre-final, used for further parameter estimation for the obtained classes). Certainly, it is desired to provide as accurate classification as possible. In particular, improvement of classification accuracy might allow slightly worse quality of an acquired image as a result of increased distance between the sensor carrier and the sensed terrain the image of which is formed.

Classification accuracy depends on numerous factors [7 - 9] including a chosen set of features, a classifier

used and its training methodology, number of classes present in a given image and their potential separability, quality and properties of original images, image pre-processing methods employed before classification, etc. This explains a great number of publications dealing with remote sensing data classification and challenges in image processing that appear each year (see [4, 10, 11] and references therein).

A general tendency in remote sensing is permanent increasing of image number and their average size. This causes problems in image transferring from a carrier to on-land center of data reception, processing and dissemination and in image storage. Considerable efforts have been undertaken to develop efficient methods and algorithms of image compression [12 - 14]. Note that compression can be lossless and lossy [15, 16]. The latter is often subdivided into visually lossless and lossy [12, 13, 17, 18].

Below, we are not interested in lossless compression since it is usually unable to provide a desired compression ratio (CR). In turn, lossy compression introduces in-

evitable distortions and they influence image classification and object recognition accuracy [14, 19 - 21].

If one has to classify a compressed image, two approaches to classifier training (most modern efficient classifiers presume training in one or another manner). The first approach assumes that training is carried out for samples that are not distorted, i.e. for original (uncompressed) images that contain the same (or a larger number) of classes that are present in a compressed image to be classified. The second approach presumes that training of a classifier is carried out for compressed data, i.e. for a part of data of a compressed image to be classified or an image compressed with similar characteristics and acquired earlier.

Both approaches have advantages and drawbacks to be discussed in the next Section. The goal of this paper is to compare these approaches. To restrict ourselves, we focus on lossy compression that introduces either invisible or not annoying distortions (if distortions are annoying, classification accuracy is usually considerably worse than required or potentially reachable; thus, it is desired to avoid such situations in practice [19]). Besides, we focus on image classification using trained neural networks. The reason for this is that neural network classifiers are usually among the best since they possess ability to work with features that have non-Gaussian distributions [19, 20]. In addition, to simplify our analysis, we consider three-channel images (which can be visualized and easily analyzed by humans) and their pixel-wise classification (to avoid extra difficulties in analysis).

This paper is organized as follows. The problem of the two-step method applied to SPIHT is defined, and its solution methodology is described in Section 2. The experiment set is presented in Section 2 as well. The results and discussion are given in Section 3. Finally, Section 4 summarizes the work.

2. Problem statement and solution methodology

a. Problem statement

Suppose we have a compressed image or several images compressed in a similar way to be classified. Assume also that we know some parameters that describe compression. This can be compression ratio obtained for the considered image or quantization step with which the image has been compressed. This means that the compressed image quality characterized by peak signal-to-noise ratio (PSNR) or other metrics (e.g., mean square error or mean absolute deviation of introduced distortions) can be predicted with quite high accuracy [18, 20] for a used technique.

Then, three strategies of compressed image classification are possible. Let describe them more in detail. According to Strategy 1, a classifier is trained in advance

using original (uncompressed, reference) data acquired by the same sensor earlier. For this strategy, there are the following advantages. First, the classifier is already trained and ready for use for a given compressed image. Second, specialists that have performed such a training, most probably, had time and, thus, were able to define all possible classes, to find image fragments for training carefully, to optimize parameters of the designed classifier and so on. Meanwhile, there are also several drawbacks of this strategy. First, distribution of features for uncompressed and compressed images differ due to distortions introduced by lossy compression. Second, distribution of features in reference and compressed images can differ for certain classes due to errors in calibration, seasonal variations of features, etc.

For the second strategy, images compressed with parameters similar to parameters of compressing an image to be classified can be used for classifier training. Then, before classification of a given compressed image, one can choose the classifier prepared for similar conditions. An advantage of this strategy is that the classifiers are ready in advance. Another positive feature is that classifiers are “adapted” to compressed images. A question is does this “adaptation” help in the sense of improving the classification accuracy? The drawbacks are that 1) the classifier training requires considerable efforts and 2) calibration errors and class feature seasonal changes might have the negative impact on classification accuracy.

Finally, according to Strategy 3, classifier training is performed just for a compressed image to be classified. Image fragments that can be recognized as belonging to given classes with confidence, are used for training. Then, the trained classifier is applied to entire image to get the classification map. A possible advantage is that training is done for a part of the same compressed data that can be then subject to classification. Then, calibration errors and seasonal changes of features have no negative impact. However, training is needed for each compressed image to be classified. This can require considerable efforts and highly qualified experts to perform the necessary operations quickly and carefully especially if time offered for classification is limited.

For the latter two strategies, one has to know do they provide benefits in classification accuracy and, if yes, how larger these benefits are. In other words, is it worth carrying out more work and spend more time for this?

Note that there are some already obtained results. The data presented in the papers [14, 18, 21] show that even if the classifier has been trained for original (uncompressed) data and then applied to compressed images, the probability of correct classification can even increase compared to classification accuracy for the corresponding uncompressed image. One reason could be the presence of the noise in original image which is partly

suppressed by lossy compression. At the same time, in most cases, the probability of correct classification usually reduces if the introduced distortions become larger [18, 20].

Thus, it is worth analyzing different “cross-classification” situations, i.e. when training is carried out for one type of data and then applied to data of another type. To partly simplify our study, we do not consider possible calibration errors and seasonal changes of features. We just analyze the original RS data and several versions of these data after compression.

b. Solution methodology

It is clear that different methods of image lossy compression introduce distortions with different characteristics. So, we are standing before dilemma – either to analyze a particular method of image lossy compression (then the obtained results will lack generality) or to analyze many (at least, several) different methods (then, a question is what coders to consider). Fortunately, an alternative approach to simulation of introduced distortions has been proposed recently [19]. It has been shown that distortions introduced by lossy compression under condition that these distortions are not too intensive usually have distribution close to Gaussian and they are practically spatially uncorrelated. This means that additive white Gaussian noise (AWGN) can be used as a simplified model of distortions for distortions introduced by lossy compression. This approach has been shown possible for many compression techniques based on discrete cosine transform where these techniques are applied to multichannel images either component-wise or in 3D manner. A positive feature of this approach to analysis of compression influence on classification is that we do not need to know the compression technique applied. In turn, a given variance of AWGN can be recalculated to coder parameters as, e.g. quantization step. This means that, in fact, we might have an approximate correspondence between AWGN variance and parameters of compression technique.

Therefore, we can easily create a set of images simulating different degrees of compression (in fact, contaminated by AWGN with different values of variance). For each image, we can then train the classifier. This classifier can be then applied to either original (noise-free) image or to noisy images with any value of noise variance. If the classifier training has been carried out for original image and then applied to noisy images, we simulate Strategy 1. If the training was performed for the same noisy image, Strategy 2 is simulated. If the training was done for the noisy image with AWGN variance that differs from noise variance for an image to be classified, we deal with Strategy 3.

For this methodology of investigations, we have to use the same image fragments for classifier training and

the same image fragments for estimation of classification accuracy.

c. Experimental set

Since CR and introduced losses depend on image characteristics, performance of compression should be analyzed for images of different complexity and, preferably, of natural scenes. Note that images with a simpler structure are usually characterized by a lower level of losses compared to images with a complex structure, where the complexity of the image can be characterized, for example, by entropy (higher entropy refers to images with a more complex structure) [18]. To analyze the effect of lossy compression (using AWGN model) on classification results, four three-channel images of the size 512×512 pixels have been used. These images have been obtained from multichannel data acquired by Sentinel-2 satellite sensor in August 2019 (see these fragments in Fig. 1). There are four visually distinguishable classes on the images: 1 – Urban, 2 – Water, 3 – Vegetation, 4 – Bare soil, where color features for many classes intersect [21]. Remote sensing images are fragments of the territory of Kharkov (images SS2 and SS4) and its environs (images SS1 and SS3), Eastern part of Ukraine.

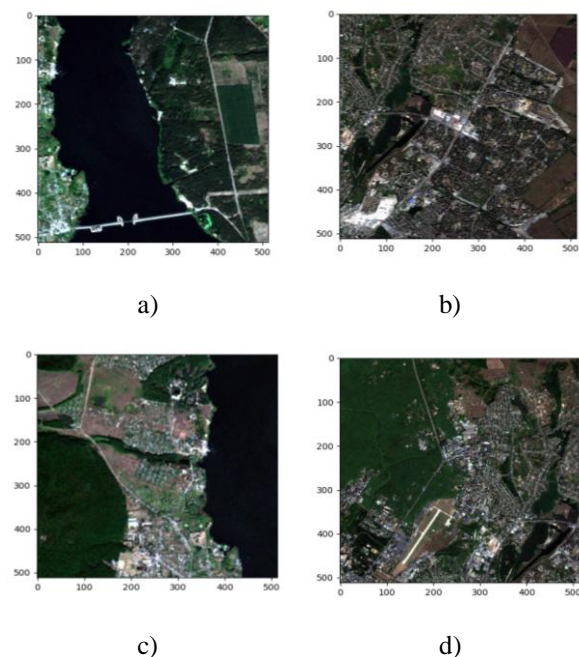


Fig. 1. Three-channel image fragments used in our analysis: SS1 (a), SS2 (b), SS3 (c), and SS4 (d)

Based on the actual data on the territory presented in these images, relatively homogeneous fragments of images representing separate classes have been identified by experts. Each of the selected fragments has been marked with a conditional color corresponding to a certain class: Urban – yellow, Water – blue, Vegetation – green, Bare soil – black. The sets of reference marked

pixels have been divided into two non-overlapping subsets: the training and control (verification) samples (Fig. 2 and 3).

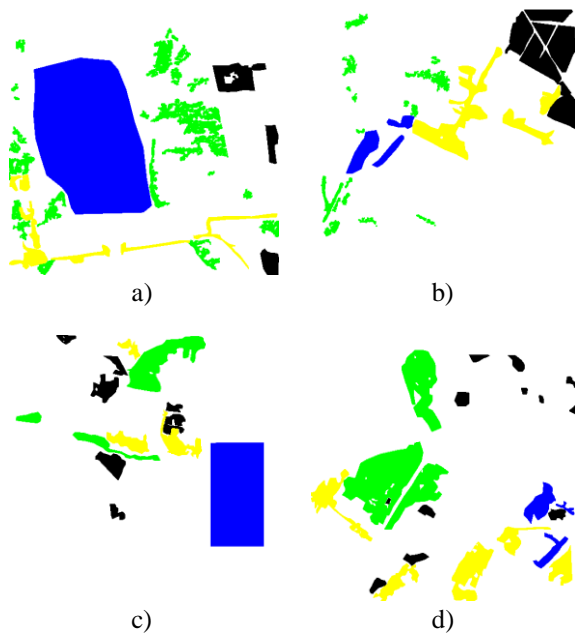


Fig. 2. Fragments used for classifier training for the images SS1 (a), SS2 (b), SS3 (c), and SS4 (d)

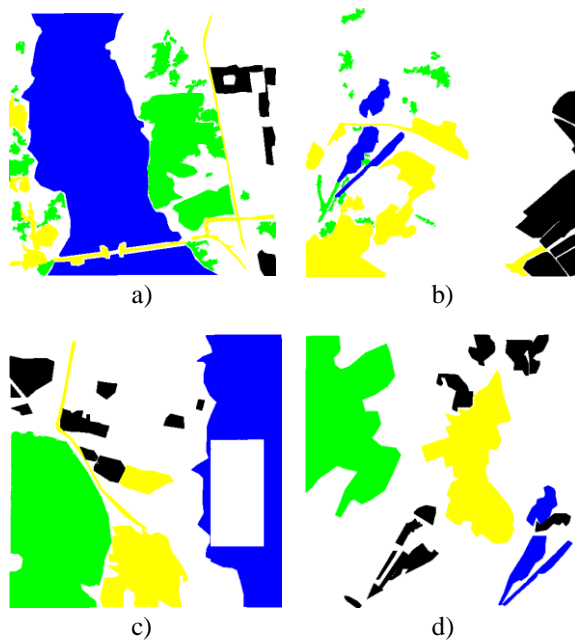


Fig. 3. Ground truth maps for the images SS1 (a), SS2 (b), SS3 (c), and SS4 (d)

The sizes of the training samples were of the order of $(4... 20) \times 10^3$ pixels, the sizes of the verification samples have been several times larger $((7... 50) \times 10^3$ pixels).

To assess the impact of the compression ratio on the quality of classification, the sets of images have been created that simulate different compression ratios, actually corrupted by AWGN with the following variance values: $\sigma^2 = 9, 25, 49, 100$ which corresponds to PSNR values from about 39 dB to 28 dB. Figures 4 and 5 show examples of these images for variance values equal to 9 and 100, respectively.



Fig. 4. Test image SS1: real life Sentinel-2 images for country-side areas in Kharkiv region, Ukraine before compression (a) and after compression with providing σ^2 equal to 9 (b) and 100 (c)

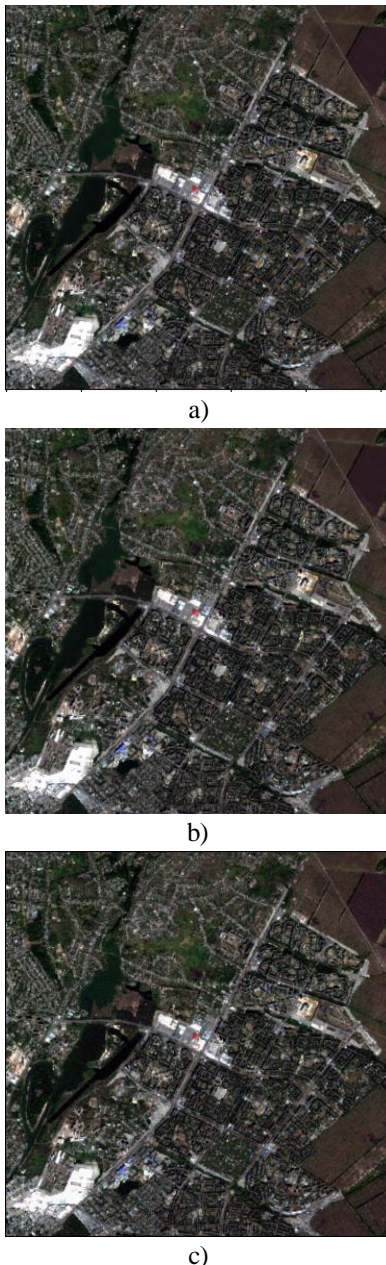


Fig. 5. Test image SS2: real life Sentinel-2 images for country-side areas in Kharkiv region, Ukraine before compression (a) and after compression with σ^2 equal to 9 (b) and σ^2 equal to 100 (c)

After obtaining feature sets (voxel values) of the considered classes, classification has been carried out using a trained neural network (NN). Nowadays, there are many neural network types and approaches to their training and optimization. For classification, we have employed a simple NN that is, nevertheless, effective for the classification of multi-channel data. The classifier used was a multilayer neural network (MLP) that uses supervised learning and backpropagation. Such neural networks have an input layer, an output layer and, at least, one hidden layer in between. With the exception of input neurons, all other neurons commonly use a non-linear ac-

tivation function. The architecture details are the following: the NN has an input layer for incoming data of three-color components, 4 hidden layers with 64, 32, 16 and 8 neurons respectively.

The optimal number of hidden layers, neurons in them, as well as the learning function were determined by experiments with a single data set. For hidden layers, the ReLU (Rectified Linear Unit) activation function is used, the output of which is 0 if the input is negative, and the input itself if this input is 0 or positive [19, 20]

$$f(x) = \max(0, x), \quad (1)$$

$$f(x) = \begin{cases} \text{max-value}, & \text{if } x \geq (\text{max-value}); \\ x, & \text{if threshold} \geq (\text{max-value}); \\ \text{negative-slope}(x - \text{threshold}), & \text{otherwise;} \end{cases} \quad (2)$$

where max-value: float ≥ 0 is the maximum activation value, by default equal to none, which means unlimited;

negative-slope: float ≥ 0 is the negative slope coefficient, by default equal to 0;

threshold: float ≥ 0 denotes the threshold value for thresholded activation, by default equal to 0.

Linear activation function is used for the output layer. The MLP is trained using the RMSProp optimizer. This optimizer takes the root of the mean squares of the gradient's overall parameters. Mathematically, it can be written as

$$u_t = -\frac{\eta}{\sqrt{G_{t-1} + \epsilon}} \cdot g_{t-1}. \quad (3)$$

We have used cross-entropy as a loss function, and F-measure as an efficiency estimation metric. This is a harmonic mean of accuracy and completeness (accuracy shows how many of the objects identified by the classifier as positive are indeed positive; completeness shows how many of the positive objects were identified by the classifier). The harmonic mean has an important property – it is close to zero if at least one of the arguments is close to zero. In the multi-class case, this is the average of the F-measure of each class with weighting depending on the average parameter [14].

Let us start by analyzing the classification results of the original three-channel images using the neural networks trained for these images.

Consider images with the simpler structure SS1 (SS3) (Fig. 1, a and Fig. 1, c). We present the classification results obtained only for the SS1 image, since for the SS3 image, which has a similar structure, the results are identical. The obtained confusion matrix is presented in Table 1. The corresponding map is given in Figure 6, a.

Table 1

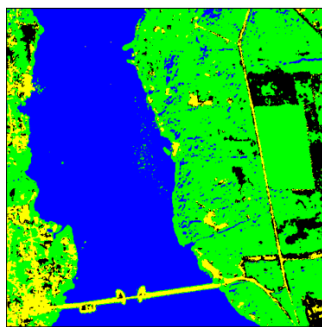
Confusion matrix for the original (noise or distortion-free) image SS1 classified by the neural networks trained for this image

Class	Probability of decision			
	Urban	Water	Vegetation	Bare soil
Urban	0.710	0.0001	0.099	0.190
Water	0.0001	0.991	0.005	0
Vegetation	0.009	0.043	0.941	0.013
Bare soil	0.044	0	0.095	0.862

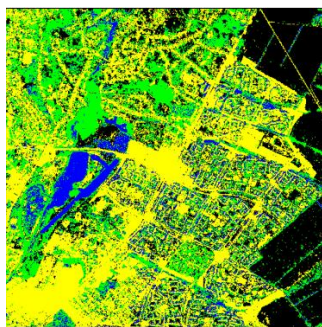
Table 2

Confusion matrix for the original (noise or distortion-free) image SS2 classified by the neural network trained for this image

Class	Probability of decision			
	Urban	Water	Vegetation	Bare soil
Urban	0.872	0.023	0.062	0.046
Water	0.081	0.613	0.381	0.009
Vegetation	0.017	0.022	0.899	0.061
Bare soil	0.022	0.005	0.068	0.913



a)



b)

Fig. 6. Classification maps for original images SS1 (a) and SS2 (b)

As one can see, the classes Water and Vegetation are recognized well. Meanwhile, there are many misclassifications for the Bare Soil and Urban classes. This is not surprising and often occurs when trying to discriminate remote sensing data for classes that are “close” to each other.

Let us consider test images SS2 (SS4) with a complex structure (Fig. 1, b and Fig. 1, d). We present the classification results obtained only for the SS2 image, since for the SS3 image, which has a similar structure, the results are identical. The obtained confusion matrix is presented in Table 2. The corresponding map is given in Fig. 6, b.

Analysis of the results shows that there are quite many misclassifications for the Vegetation and, especially, Water classes. Thus, the Water and Vegetation classes are recognized worse than in the previous case (Table 1). However, the Urban and Bare soil classes are better recognized than in the previous case with probabilities equal to 0.872 and 0.913, respectively. The total (aggregate) probabilities for SS1 and SS2 images’ correct classification are equal to 0.95 and 0.86, respectively. Thus, more complex structure image is classified worse than the simpler structure one (the same holds for the images SS3 and SS4).

3. Obtained results and discussion

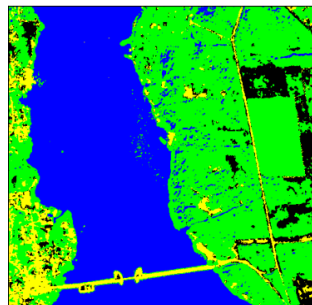
Let us consider the classification results according to strategy 1, i.e. training is carried out using the original image and classification if performed for images with artificially added noise that simulates distortions due to compression. This strategy is considered in detail in [18]. Let us present the results of image classification SS1 and SS2 for different variances. Particular classes’ and total probabilities of correct classification for the image SS1 with different noise intensities are represented in Table 3.

Table 3

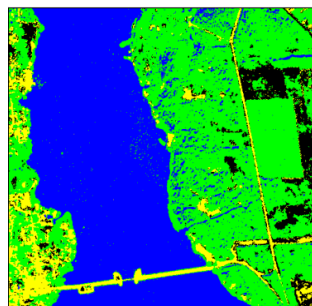
Particular class and total probabilities of correct classification for the image SS1 with different noise intensities – Strategy 1

Class	Original	σ^2			
		9	25	49	100
Urban	0.82	0.81	0.81	0.79	0.75
Water	0.99	0.98	0.96	0.94	0.88
Vegetation	0.93	0.91	0.87	0.81	0.70
Bare soil	0.77	0.76	0.74	0.70	0.64
Total	0.92	0.91	0.90	0.88	0.81

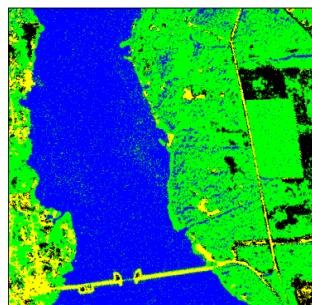
The corresponding maps are given in Figure 7. The presented results demonstrate that, firstly, the total probabilities of correct classification have a steady tendency to decrease with increasing the noise variance (distortion level). The decrease may be acceptable for $\sigma^2 = 25$, but it becomes inappropriate for larger σ^2 .



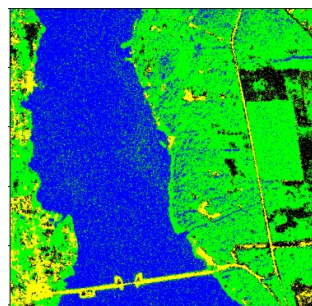
a)



b)



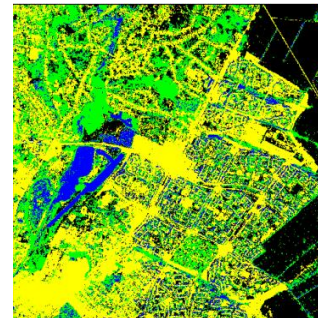
c)



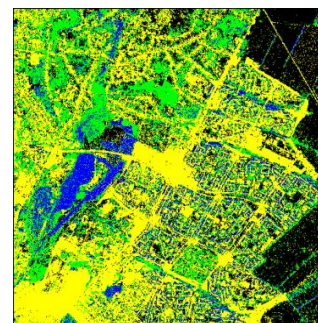
d)

Fig. 7. Classification results for the SS1 image for original (a) and noisy images: b – $\sigma^2=9$; c – $\sigma^2=25$; d – $\sigma^2=49$

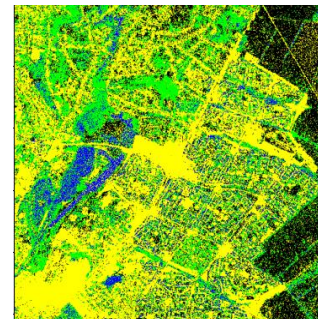
The reduction of classification accuracy also depends on the image complexity. For example, the classification results for the SS2 test image (Fig. 8), presented in Table 4, show a decrease in all particular class probabilities, as well as the total probabilities of correct classification with increasing the noise intensity.



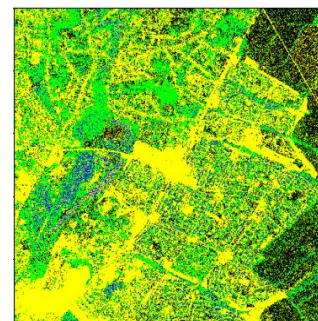
a)



b)



c)



d)

Fig. 8. Classification results for SS2 fragment maps for original (a) and noisy images: (b – $\sigma^2=9$; c – $\sigma^2=25$; d – $\sigma^2=49$)

Table 4
Particular class and total probabilities of correct classification for the image SS2 with different noise intensities – Strategy 1

Class	Original	σ^2			
		9	25	49	100
Urban	0.92	0.91	0.87	0.84	0.81
Water	0.72	0.70	0.60	0.50	0.24
Vegetation	0.64	0.60	0.57	0.51	0.42
Bare soil	0.91	0.86	0.82	0.74	0.61
Total	0.86	0.83	0.78	0.74	0.65

The decrease may be considered acceptable for $\sigma^2 = 9$, but it becomes too large for larger σ^2 . Thus, we come to the need to provide PSNR of compressed data of the order of 38 dB and higher, i.e. ensuring the invisibility of the introduced distortions (usually this happens if the PSNR exceeds 36 dB).

Consider the classification results according to strategy 3, i.e. both the training and classification are performed using an image with the same introduced noise variance value. The classification results for the SS1 and SS2 images with different noise intensities are represented in Tables 5 and 6. The corresponding maps are given in Fig. 9.

Table 5
Particular class and total probabilities of correct classification for the image SS1 with different noise intensities – Strategy 3

Class	σ^2			
	9	25	49	100
Urban	0.81	0.80	0.67	0.78
Water	0.98	0.98	0.96	0.95
Vegetation	0.91	0.90	0.84	0.80
Bare soil	0.74	0.74	0.66	0.67
Total	0.94	0.94	0.90	0.89

The presented results demonstrate that, firstly, the total probabilities of correct classification only slightly decrease with increasing the noise variance. In this case, the reduction remains acceptable even at $\sigma^2 = 49$ regardless of the complexity of the image. For example, for

$\sigma^2 = 49$, for Strategy 1 the total probabilities of correct classification are equal to 0.88 and 0.74 for the images SS1 and SS2, respectively. Meanwhile, for Strategy 3, these probabilities are equal to 0.90 and 0.80, i.e. sufficiently larger.

Table 6
Particular class and total probabilities of correct classification for the image SS2 with different noise intensities – Strategy 3

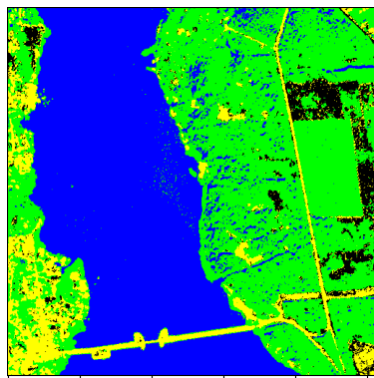
Class	σ^2			
	9	25	49	100
Urban	0.91	0.90	0.87	0.87
Water	0.72	0.77	0.75	0.77
Vegetation	0.59	0.60	0.55	0.49
Bare soil	0.86	0.85	0.82	0.78
Total	0.83	0.83	0.80	0.78

Thus, the main feature of this strategy - "adaptability" to compressed images - leads to a noticeable improvement in classification accuracy for compressed images compared to Strategy 1, especially if distortions due to lossy compression are considerable.

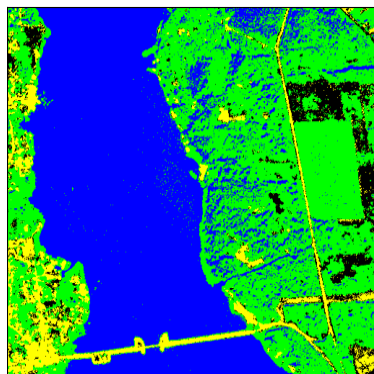
Finally, consider the results of image classification in accordance with Strategy 2, which implies both learning and classification for both compressed images, but characterized by different degrees of compression. Let us illustrate the results with the data presented in Figures 10 – 13 and in Tables 7 and 8.

The classification results show that if the values of the variances for the image we are training on and the image we are classifying are close, then the overall probabilities of correct classification are only slightly reduced compared to Strategy 3. Otherwise, significant losses are possible. At the same time, in images with a more complex structure, such losses are greater than in "simple" images.

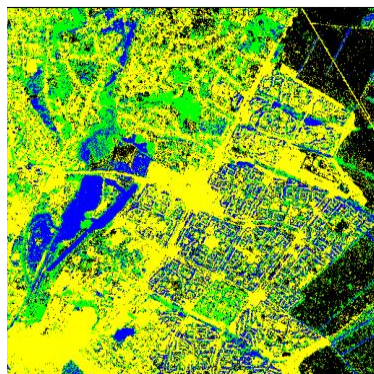
The dependences of the classification accuracy for compressed images on the chosen classification strategy is given in Fig. 14 for the images SS1, SS2, SS3 and SS4. These dependences show that Strategy 3 provides the best results. The results of Strategy 2 are close to it when choosing the classifier trained for images compressed with similar parameters (introduced losses). Strategy 1 is the worst and its use is especially undesired for images compressed with large CR and/or complex structure images.



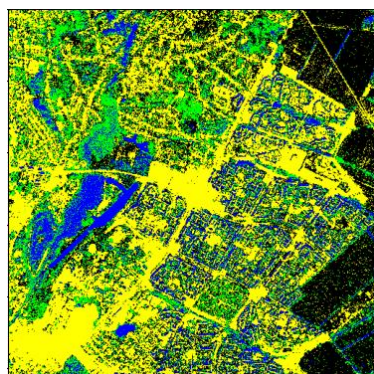
a)



b)

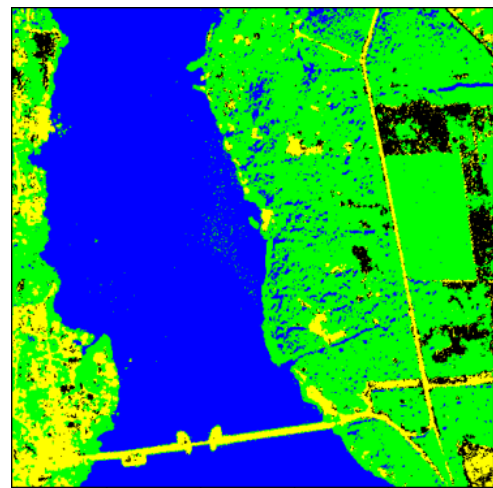


c)

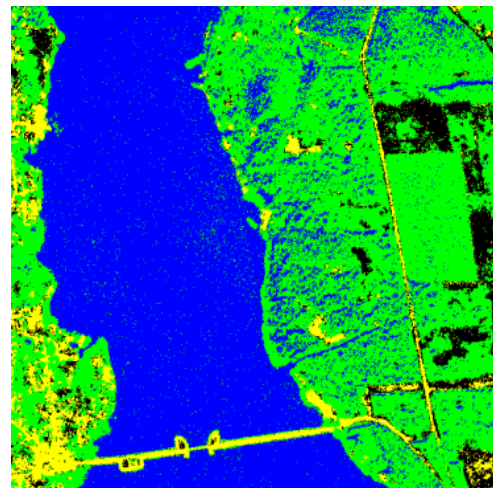


d)

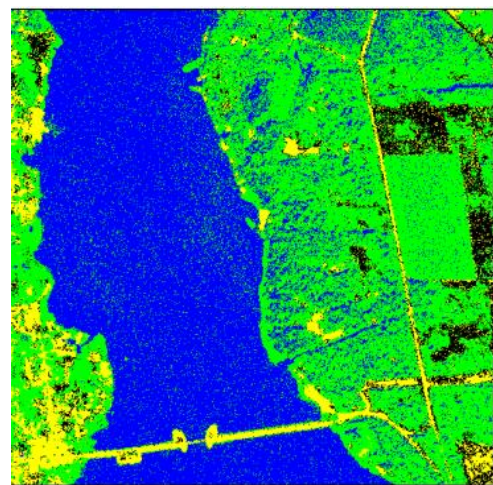
Fig. 9. Classification results for the SS1 and SS2 images maps for noisy ($\sigma^2=9$ (a) and (c); $\sigma^2=49$ (b) and (d)) images respectively for Strategy 3



a)

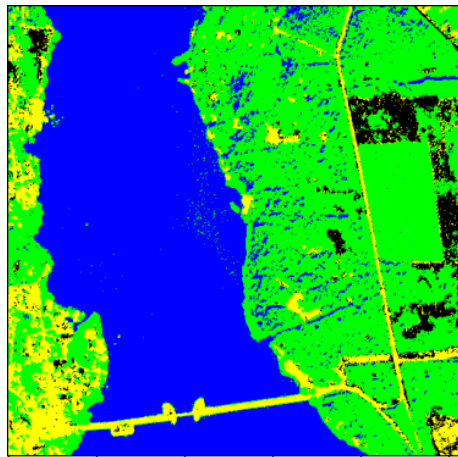


b)

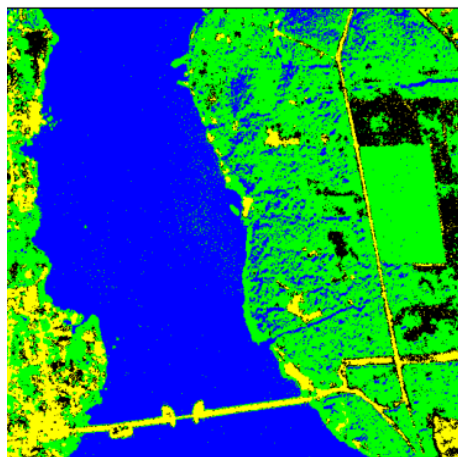


c)

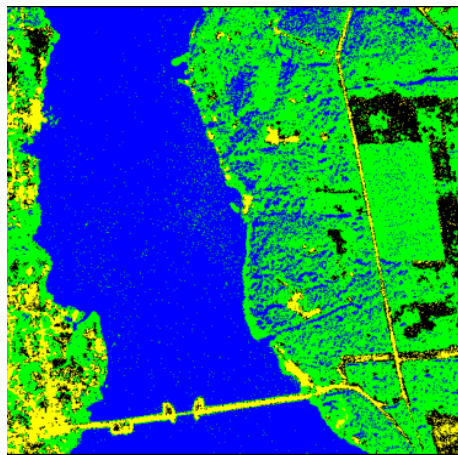
Fig. 10. Classification results for the SS1 image for noisy ($\sigma^2=9$ (a); $\sigma^2=49$ (b) and $\sigma^2=100$ (c)) images, respectively, for Strategy 2 with noisy training image ($\sigma^2=9$)



a)



b)



c)

Fig. 11. Classification results for the SS1 image for noisy ($\sigma^2=9$ (a); $\sigma^2=49$ (b) and $\sigma^2=100$ (c)) images, respectively, for Strategy 2 with noisy training image ($\sigma^2=49$)

Table 7

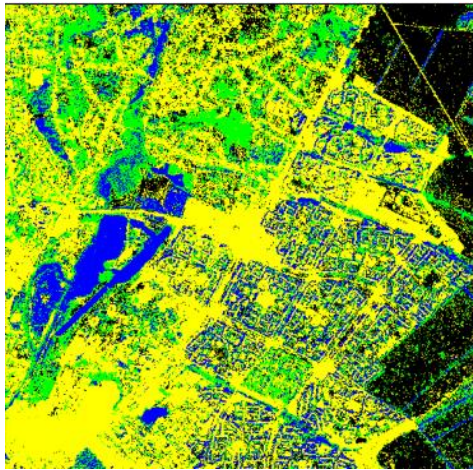
Particular class and total probabilities of correct classification for the image SS1 with different noise intensities – Strategy 2

Class	$\sigma^2 = 9$	$\sigma^2 = 25$	$\sigma^2 = 49$	$\sigma^2 = 100$
$\sigma^2 = 9$ (training image)				
Urban	0.81	0.81	0.80	0.76
Water	0.98	0.97	0.96	0.95
Vegetation	0.91	0.89	0.86	0.80
Bare soil	0.74	0.71	0.71	0.66
Total	0.94	0.93	0.91	0.88
$\sigma^2 = 49$ (training image)				
Urban	0.82	0.80	0.67	0.75
Water	0.98	0.98	0.96	0.96
Vegetation	0.92	0.90	0.84	0.84
Bare soil	0.76	0.74	0.66	0.68
Total	0.94	0.93	0.90	0.90

Table 8

Particular class and total probabilities of correct classification for the image SS2 with different noise intensities – Strategy 2

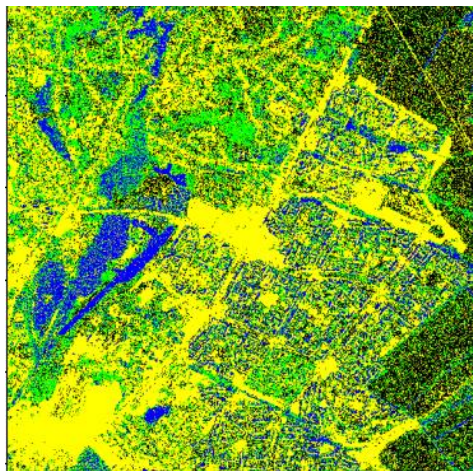
Class	$\sigma^2 = 9$	$\sigma^2 = 25$	$\sigma^2 = 49$	$\sigma^2 = 100$
$\sigma^2 = 9$ (training image)				
Urban	0.91	0.88	0.87	0.82
Water	0.72	0.75	0.70	0.71
Vegetation	0.59	0.59	0.53	0.49
Bare soil	0.86	0.84	0.79	0.70
Total	0.83	0.81	0.78	0.73
$\sigma^2 = 49$ (training image)				
Urban	0.89	0.89	0.87	0.87
Water	0.78	0.80	0.75	0.69
Vegetation	0.64	0.58	0.55	0.48
Bare soil	0.86	0.83	0.82	0.76
Total	0.83	0.82	0.80	0.77



a)

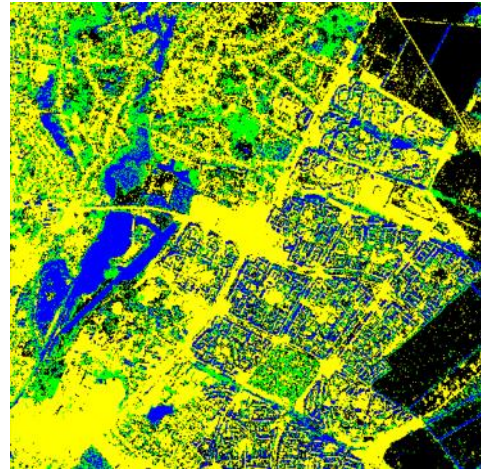


b)

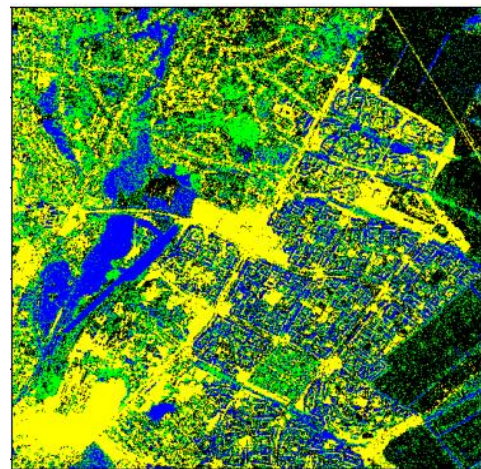


c)

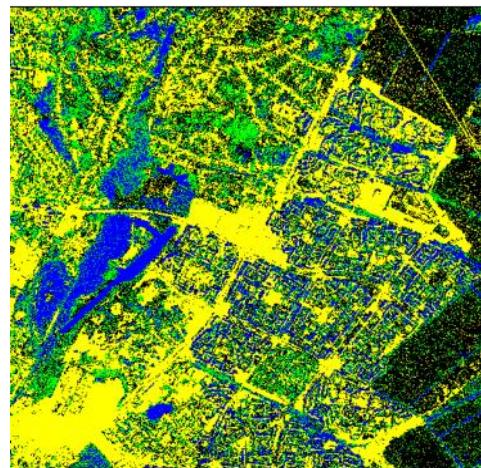
Fig. 12. Classification results for the SS2 image for noisy ($\sigma^2=9$ (a); $\sigma^2=49$ (b) and $\sigma^2=100$ (c)) images, respectively, for Strategy 2 with noisy training image ($\sigma^2=9$)



a)



b)



c)

Fig. 13. Classification results for the SS2 image for noisy ($\sigma^2=9$ (a); $\sigma^2=49$ (b) and $\sigma^2=100$ (c)) images respectively for Strategy 2 with noisy training image ($\sigma^2=49$)

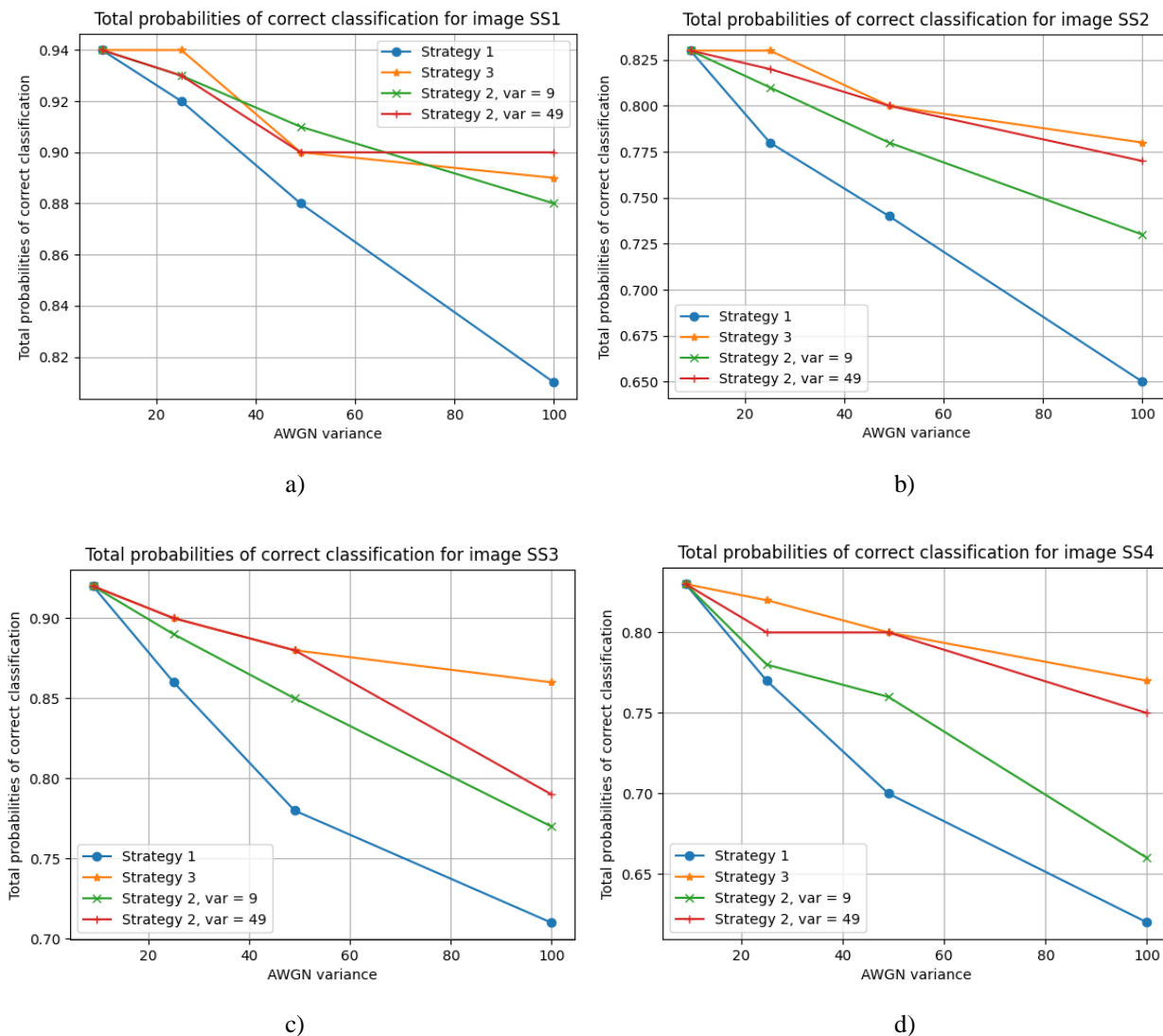


Fig. 14. Classification results for SS1 (a), SS2 (b), SS3 (c) and SS4 (d) images

4. Conclusions

We have considered three strategies to NN classifier learning for processing compressed three-channel remote sensing images. According to Strategy 1, training is done for distortion-free data. It might seem slightly surprising, but this Strategy occurs less efficient than training for compressed images (Strategies 2 and 3), especially if an image to be classified is compressed with a quite large CR and/or for complex structure images. In turn, classifier training is expedient for compressed images (in general, Strategy 2), especially if compression parameters (level of introduced distortions) are practically the same as for an image the classifier is applied to. This means that in practice one might carry out preliminary training of several classifiers for several levels of distortions. As the simplest case, it is possible to have two pre-trained classifiers, one for visually lossless compression (PSNR about 37 dB) and one for lossy compression with visually

noticeable distortions (PSNR about 32 dB). Note that PSNR for compressed image can be determined for at the stage of its compression and such PSNR can be added to file heading as auxiliary information.

One opportunity to improve classification not studied in this paper is to perform post-classification that is able to incorporate knowledge (classification results) from neighbor pixels [22, 23].

Contributions of authors: conceptualization – Vladimir Lukin, Galina Proskura, Oleksii Rubel; methodology – Vladimir Lukin, Galina Proskura; formulation of tasks – Vladimir Lukin; analysis – Vladimir Lukin, Galina Proskura, Oleksii Rubel; development of model – Vladimir Lukin, Galina Proskura, Oleksii Rubel; software – Galina Proskura; verification – Vladimir Lukin, Oleksii Rubel; analysis of results – Vladimir Lukin, Galina Proskura, Oleksii Rubel; visualization – Galina Proskura; writing – original

draft preparation – **Vladimir Lukin, Galina Proskura**;
writing – review and editing – **Vladimir Lukin,**
Oleksii Rubel.

All the authors have read and agreed to the published version of the manuscript.

References (GOST 7.1:2006)

1. *Potential Applications of the Sentinel-2 Multi-spectral Sensor and the ENMAP hyperspectral Sensor in Mineral Exploration [Text]* / C. Mielke, N. K. Boshce, C. Rogass, K. Segl, C. Gauert, H. Kaufmann // *EARSeL eProceedings*. – 2014. – Vol. 13, No. 2. – P. 93-102. DOI: 10.12760/01-2014-2-07.
2. *Crop inventory at regional scale in Ukraine: Developing in season and end of season crop maps with multi-temporal optical and SAR satellite imagery [Text]* / N. Kussul, M. Lavreniuk, A. Shelestov, S. Skakun // *European Journal of Remote Sensing*. – 2018. – Vol. 51, Iss. 1. – P. 627-636. DOI: 10.1080/22797254.2018.1454265.
3. *Zhong, P. Multiple-Spectral-Band CRFs for Denoising Junk Bands of Hyperspectral Imagery [Text]* / P. Zhong, R. Wang // *IEEE Transactions on Geoscience and Remote Sensing*. – 2013. – Vol. 51, Iss. 4. – P. 2269-2275. DOI: 10.1109/TGRS.2012.2209656.
4. *Parcel-Based Crop Classification in Ukraine Using Landsat-8 Data and Sentinel-1A Data [Text]* / N. Kussul, G. Lemoine, F. J. Gallego, S. V. Skakun, M. Lavreniuk, A. Yu. Shelestov // *IEEE Journal of Selected Topics in Applied Earth Observations and Remote Sensing*. – 2016. – Vol. 9, Iss. 6. – P. 2500-2508. DOI: 10.1109/JSTARS.2016.2560141.
5. *Automatic remotely sensed image classification in a grid environment based on the maximum likelihood method [Text]* / J. Sun, J. Yang, C. Zhang, W. Yun, J. Qu // *Mathematical and Computer Modelling*. – 2013. – Vol. 58, Iss. 3-4. – P. 573-581. DOI: 10.1016/j.mcm.2011.10.063.
6. *Sisodia, P. S. Analysis of Supervised Maximum Likelihood Classification for remote sensing image [Text]* / P. S. Sisodia, V. Tiwari, A. Kumar // *International Conference on Recent Advances and Innovations in Engineering (ICRAIE-2014)*. – 2014. – P. 1-4. DOI: 10.1109/ICRAIE.2014.6909319.
7. *Sajjad, H. Future Challenges and Perspective of Remote Sensing Technology [Text]* / H. Sajjad, P. Kumar // *In Applications and Challenges of Geospatial Technology* ; P. Kumar, M. Rani, P. Chandra, H. Sajjad, B. Chaudhary (eds.). – Springer, Cham, 2019. – P. 275-277. DOI: 10.1007/978-3-319-99882-4_16.
8. *Hyperspectral Remote Sensing Data Analysis and Future Challenges [Text]* / J. M. Bioucas-Dias, A. Plaza, G. Camps-Valls, P. Scheunders, N. Nasrabadi, J. Chanussot // *IEEE Geoscience and Remote Sensing Magazine*. – 2013. – Vol. 1, Iss. 2. – P. 6-36. DOI: 10.1109/MGRS.2013.2244672.
9. *Oh, H. Visually lossless JPEG 2000 for remote image browsing [Text]* / H. Oh, A. Bilgin, M. Marcellin // *Information*. – 2016. – Vol. 7, Iss. 3. – Article No. 45. DOI: 10.3390/info7030045.
10. *Spectral distortion in lossy compression of hyperspectral imagery [Text]* / B. Aiazzi, L. Alparone, S. Baronti, C. Lastris, L. Santurri, M. Selva // *IEEE International Geoscience and Remote Sensing Symposium (IGARSS 2003). Proceedings (IEEE Cat. No. 03CH37477)*. – 2003. – P. 1817-1819. DOI: 10.1109/IGARSS.2003.1294260.
11. *Effects of JPEG and JPEG2000 lossy compression on remote sensing image classification for mapping crops and forest areas [Text]* / A. Zabala, X. Pons, R. Diaz-Delgado, F. Garcia, F. Auli-Llinas, J. Serra-Sagrista // *IEEE International Symposium on Geoscience and Remote Sensing*. – 2006. – P. 790-793. DOI: 10.1109/IGARSS.2006.203.
12. *Sayood, K. Introduction to data compression [Text]* / K. Sayood ; Fifth Edition. – San Francisco : Morgan Kaufmann, 2018. DOI: 10.1016/C2015-0-06248-7.
13. *Hussain, A. J. Image compression techniques: A survey in lossless and lossy algorithms [Text]* / A. J. Hussain, A. Al-Fayadh, N. Radi // *Neurocomputing*. – 2018. – Vol. 300. – P. 44-69. DOI: 10.1016/j.neucom.2018.02.094.
14. *Deep learning-based picture-wise just noticeable distortion prediction model for image compression [Text]* / H. Liu, Y. Zhang, H. Zhang, et al. // *IEEE Transactions on Image Processing*. – 2019. – Vol. 29. – P. 641-656. DOI: 10.1109/TIP.2019.2933743.
15. *Li, F. Two-step providing of desired quality in lossy image compression by SPIHT [Text]* / F. Li, S. Krivenko, V. Lukin // *Radioelectronic and computer systems*. – 2020. – No. 2(94). – P. 22-32. DOI: 10.32620/reks.2020.2.02.
16. *Ozah, N. Compression improves image classification accuracy [Text]* / N. Ozah, A. Kolokolova // *Advances in Artificial Intelligence. Canadian AI 2019. Lecture Notes in Computer Science*. – Springer, Cham, 2019. – Vol. 11489. – P. 525-530. DOI: 10.1007/978-3-030-18305-9_55.
17. *Satellite image remote sensing for identifying aircraft using SPIHT and NSCT [Text]* / S. Doss, S. Pal, D. Akila, et al. // *IEEE Signal processing magazine*. – 2020. – Vol. 7, No. 5. – P. 631-634. DOI: 10.31838/jcr.07.05.130.
18. *Image Classification Accuracy Analysis for Three-channel Remote Sensing Data [Electronic resource]* / F. Li, V. Lukin, G. Proskura, I. Vasilyeva, G. Chernova // *Proceedings of the conference "Intelligent Information technologies and systems of information security" IntellITSIS-2022, March 23–25, 2022,*

Ukraine. – 15 p. – Available at: <http://ceur-ws.org/Vol-3156/paper39.pdf>. – 10.04.2022.

19. Ustuner, M. Comparison of Neural Network and ISODATA classifiers for Land Cover Assessment Using Optical Data [Text] / M. Ustuner, F. B. Sanli // FIG Commission 3 Workshop 2012 Spatial Information, Informal Development, Property and Housing, Athens, Greece, 10-14 December 2012. – P. 1-7.

20. Analysis of Classification Quality of DAT-Based Compression Images [Text] / G. Proskura, V. Makarichev, O. Rubel, V. Lukin // IEEE 16th International Conference on Advanced Trends in Radioelectronics, Telecommunications and Computer Engineering (TCSET). – 2022. – P. 233-238. DOI: 10.1109/TCSET55632.2022.9766942.

21. Lossy Compression of Multichannel Remote Sensing Images with Quality Control [Text] / V. Lukin, I. Vasilyeva, S. Krivenko, F. Li, S. Abramov, O. Rubel, B. Vozel, K. Chehdi, K. Egiazarian // Remote Sensing. – 2020. – Vol. 12, Iss. 22. – Article No. 3840. DOI: 10.3390/rs12223840.

22. Васильева, И. К. Анализ методов постклассификационной обработки многоканальных изображений [Текст] / И. К. Васильева, В. В. Лукин // Радіоелектронні і комп'ютерні системи. – 2019. – № 1(89). – С. 17-28. DOI: 10.32620/reks.2019.1.02.

23. Classification of Compressed Multichannel Images and Its Improvement [Text] / G. Proskura, I. Vasilyeva, F. Li, V. Lukin // 30th International Conference Radioelektronika 2020, April 2020, Bratislava, Slovakia. – 2020. – P. 1-6. DOI: 10.1109/RADIOELEKTRONIKA49387.2020.9092371.

References (BSI)

1. Mielke, C., Boshce, N. K., Rogass, C., Segl, K., Gauert, C., Kaufmann, H. Potential Applications of the Sentinel-2 Multispectral Sensor and the ENMAP hyperspectral Sensor in Mineral Exploration. *EARSeL eProceedings*, 2014, vol. 13, no. 2, pp. 93-102. DOI: 10.12760/01-2014-2-07.

2. Kussul, N., Lavreniuk, M., Shelestov, A., Skakun, S. Crop inventory at regional scale in Ukraine: Developing in season and end of season crop maps with multi-temporal optical and SAR satellite imagery. *European Journal of Remote Sensing*, 2018, vol. 51, iss. 1, pp. 627-636. DOI: 10.1080/22797254.2018.1454265.

3. Zhong, P., Wang, R. Multiple-Spectral-Band CRFs for Denoising Junk Bands of Hyperspectral Imagery. *IEEE Transactions on Geoscience and Remote Sensing*, 2013, vol. 51, iss. 4, pp. 2269-2275. DOI: 10.1109/TGRS.2012.2209656.

4. Kussul, N., Lemoine, G., Gallego, F. J., Skakun, S. V., Lavreniuk, M., Shelestov, A. Yu. Parcel-Based Crop Classification in Ukraine Using Landsat-8 Data and

Sentinel-1A Data. *IEEE Journal of Selected Topics in Applied Earth Observations and Remote Sensing*, 2016, vol. 9, iss. 6, pp. 2500-2508. DOI: 10.1109/JSTARS.2016.2560141.

5. Sun, J., Yang, J., Zhang, C., Yun, W., Qu, J. Automatic remotely sensed image classification in a grid environment based on the maximum likelihood method. *Mathematical and Computer Modelling*, 2013, vol. 58, iss. 3-4, pp. 573-581. DOI: 10.1016/j.mcm.2011.10.063.

6. Sisodia, P. S., Tiwari, V., Kumar, A. Analysis of Supervised Maximum Likelihood Classification for remote sensing image. *International Conference on Recent Advances and Innovations in Engineering (ICRAIE-2014)*, 2014, pp. 1-4. DOI: 10.1109/ICRAIE.2014.6909319.

7. Sajjad, H., Kumar, P. Future Challenges and Perspective of Remote Sensing Technology. In *Applications and Challenges of Geospatial Technology*, P. Kumar, M. Rani, P. Chandra, H. Sajjad, B. Chaudhary (eds.), Springer, Cham, 2019, pp. 275-277. DOI: 10.1007/978-3-319-99882-4_16.

8. Bioucas-Dias, J. M., Plaza, A., Camps-Valls, G., Scheunders, P., Nasrabadi, N., Chanussot, J. Hyperspectral Remote Sensing Data Analysis and Future Challenges. *IEEE Geoscience and Remote Sensing Magazine*, 2013, vol. 1, iss. 2, pp. 6-36. DOI: 10.1109/MGRS.2013.2244672.

9. Oh, H., Bilgin, A., Marcellin, M. Visually lossless JPEG 2000 for remote image browsing. *Information*, 2016, vol. 7, iss. 3, article no. 45. DOI: 10.3390/info7030045.

10. Aiazzi, B., Alparone, L., Baronti, S., Lastri, C., Santurri, L., Selva, M. Spectral distortion in lossy compression of hyperspectral imagery. *IEEE International Geoscience and Remote Sensing Symposium (IGARSS 2003)*. Proceedings (IEEE Cat. No. 03CH37477), 2003, pp. 1817-1819. DOI: 10.1109/IGARSS.2003.1294260.

11. Zabala, A., Pons, X., Díaz-Delgado, Garcia, R., Auli-Llinas, F. F., Serra-Sagrista, J. Effects of JPEG and JPEG2000 lossy compression on remote sensing image classification for mapping crops and forest areas. *IEEE International Symposium on Geoscience and Remote Sensing*, 2006, pp. 790-793. DOI: 10.1109/IGARSS.2006.203.

12. Sayood, K. *Introduction to data compression. Fifth Edition*. San Francisco, Morgan Kaufmann Publ., 2018. DOI: 10.1016/C2015-0-06248-7.

13. Hussain, A. J., Al-Fayadh, A., Radi, N. Image compression techniques: A survey in lossless and lossy algorithms. *Neurocomputing*, 2018, vol. 300, pp. 44-69. DOI: 10.1016/j.neucom.2018.02.094.

14. Liu, H., Zhang, Y., Zhang, H. et al. Deep learning-based picture-wise just noticeable distortion prediction model for image compression. *IEEE Transactions on*

Image Processing, 2019, vol. 29, pp. 641-656. DOI: 10.1109/TIP.2019.2933743.

15. Li, F., Krivenko, S., Lukin, V. Two-step providing of desired quality in lossy image compression by SPIHT. *Radioelectronic and computer systems*, 2020, no. 2(94), pp. 22-32. DOI: 10.32620/reks.2020.2.02.

16. Ozah, N., Kolokolova, A. Compression improves image classification accuracy. *Advances in Artificial Intelligence. Canadian AI 2019. Lecture Notes in Computer Science*. Springer, Cham, 2019, vol. 11489, pp. 525-530. DOI: 10.1007/978-3-030-18305-9_55.

17. Doss, S., Pal, S., Akila, D. et al. Satellite image remote sensing for identifying aircraft using SPIHT and NSCT. *IEEE Signal processing magazine*, 2020, vol. 7, no. 5, pp. 631-634. DOI: 10.31838/jcr.07.05.130.

18. Li, F., Lukin, V., Proskura, G., Vasilyeva, I., Chernova, G. Image Classification Accuracy Analysis for Three-channel Remote Sensing Data. *Proceedings of the conference "Intelligent Information technologies and systems of information security" IntelITSIS-2022, March 23-25, 2022, Ukraine*. 15 p. Available at: <http://ceur-ws.org/Vol-3156/paper39.pdf>. (accessed 10.04.2022).

19. Ustuner, M., Sanli, F. B. Comparison of Neural Network and ISODATA classifiers for Land Cover Assessment Using Optical Data. *FIG Commission 3 Workshop 2012 Spatial Information, Informal Development, Property and Housing*, 2012, pp. 1-7.

20. Proskura, G., Makarichev, V., Rubel, O., Lukin, V. Analysis of Classification Quality of DAT-Based Compression Images. *IEEE 16th International Conference on Advanced Trends in Radioelectronics, Telecommunications and Computer Engineering (TCSET)*, 2022, pp. 233-238. DOI: 10.1109/TCSET55632.2022.9766942.

21. Lukin, V., Vasilyeva, I., Krivenko, S., Li, F., Abramov, S., Rubel, O., Vozel, B., Chehdi, K., Egiazarian, K. Lossy Compression of Multichannel Remote Sensing Images with Quality Control. *Remote Sensing*, 2020, vol. 12, iss. 22, article no. 3840. DOI: 10.3390/rs12223840.

22. Vasil'eva, I. K., Lukin, V. V. Analiz metodov postklassifikatsionnoi obrabotki mnogokanal'nykh izobrazhenii [Multichannel images post-classification processing techniques analysis]. *Radioelectronic and computer systems*, 2019, no. 1(89), pp. 17-28. DOI: 10.32620/reks.2019.1.02.

23. Proskura, G., Vasilyeva, I., Li, F., Lukin, V. Classification of Compressed Multichannel Images and Its Improvement. *30th International Conference Radioelektronika 2020*, April 2020, Bratislava, Slovakia, 2020, pp. 1-6. DOI: 10.1109/RADIOELEKTRONIKA 49387.2020.9092371.

Надійшла до редакції 17.04.2022, розглянута на редколегії 25.08.2022

ПРО МЕТОДОЛОГІЇ НАВЧАННЯ КЛАСИФІКАТОРІВ ІЗ ЗАСТОСУВАННЯМ СТИСНЕНИХ ЗОБРАЖЕНЬ ДИСТАНЦІЙНОГО ЗОНДУВАННЯ

Г. А. Проскура, О. С. Рубель, В. В. Лукін

В даний час зображення дистанційного зондування Землі знайшли безліч застосувань. Найчастіше кінцевим або проміжним результатом їх обробки є класифікаційна карта. Такі карти зазвичай отримують за допомогою попередньо навченого класифікатора, і однією з вимог, що пред'являються до них, є їх точність. Основним предметом статті є чинники, що визначають цю точність. Основними з них є якість даних ДЗЗ та тип класифікатора, параметри та підхід до навчання. Якість зображення може погіршитися через кілька факторів. Одним з них є спотворення, що вносяться стиском з втратами, який широко використовуються у зв'язку з величезним обсягом даних і необхідністю значно зменшити їх обсяг на етапах передачі, зберігання та/або розповсюдження. З цієї причини основною метою статті є спільний розгляд класифікації та стиснення із втратами. Зокрема, це означає, що навчання класифікатора може проводитися як для вихідних (нестиснених, стиснутих без втрат) зображень (за їх наявності), так і для наявних стислих даних (пропонованих користувачеві для класифікації та подальшого аналізу). Завдання цієї статті полягає в тому, щоб розглянути та порівняти ці два варіанти. Перший - це навчання класифікатора на вихідних зображеннях і подальше його застосування до стиснених даних, де зображення можуть бути стиснуті з різним ступенем стиснення. Другий варіант - використання навчання класифікатора для стиснених зображень, де параметри стиснення для навчальних даних можуть бути приблизно такими, як і для зображень, до яких застосовується класифікатор. Основний результат полягає у тому, що остання методологія здатна забезпечити певні переваги проти навчання класифікатора для вихідних даних, якщо необхідно класифікувати стислі дані дистанційного зондування Землі. Результати отримані для класифікатора на основі нейронної згорткової мережі. Як зображення для навчання та перевірки використовуються чотири реально існуючі триканальні (видимий діапазон) зображення Sentinel-2" Харкова та Харківської області, які характеризуються різною за складністю структурою та містять чотири основні

класи об'єктів на місцевості. Надано практичні рекомендації. Як **висновки** можна констатувати, що варто навчати класифікатори для декількох ступенів стиснення і з особливою обережністю стискати зображення складної структури.

Ключові слова: стиснення з втратами; триканальні зображення; класифікація; нейронна мережа; навчальні дані.

Проскура Галина Анатоліївна – канд. техн. наук, доц. каф. інформаційно-комунікаційних технологій ім. О. О. Зеленського, Національний аерокосмічний університет ім. М. Є. Жуковського «Харківський авіаційний інститут», Харків, Україна.

Рубель Олексій Сергійович – канд. техн. наук, доц. каф. інформаційно-комунікаційних технологій ім. О. О. Зеленського, Національний аерокосмічний університет ім. М. Є. Жуковського «Харківський авіаційний інститут», Харків, Україна.

Лукін Володимир Васильович – д-р техн. наук, проф., зав. каф. інформаційно-комунікаційних технологій ім. О. О. Зеленського, Національний аерокосмічний університет ім. М. Є. Жуковського «Харківський авіаційний інститут», Харків, Україна.

Galina Proskura – Candidate of Technical Sciences, Associate Professor of the Department of Information-Communication Technologies named after O. O. Zelensky, National Aerospace University "Kharkiv Aviation Institute", Kharkiv, Ukraine,
e-mail: g.proskura@khai.edu, ORCID: 0000-0001-8960-0421, ResearcherID: E-8162-2019,
Scopus Author ID: 26028048100.

Oleksii Rubel – Candidate of Technical Sciences, Associate Professor of the Department of Information-Communication Technologies named after O. O. Zelensky, National Aerospace University "Kharkiv Aviation Institute", Kharkiv, Ukraine,
e-mail: o.rubel@khai.edu, ORCID: 0000-0001-6206-3988, ResearcherID: O-5309-2014,
Scopus Author ID: 56925032900.

Vladimir Lukin – Doctor of Technical Sciences, Professor, Head of the Department of Information-Communication Technologies named after O. O. Zelensky, National Aerospace University "Kharkiv Aviation Institute", Kharkiv, Ukraine,
e-mail: lukin@ai.kharkov.com, ORCID: 0000-0002-1443-9685.